A mutation in POLR3E impairs antiviral immune response and RNA polymerase III

Aravind Ramanathan[a,1], Michael Weintraub[b,1,2], Natalie Orlovetskie[a,1], Raphael Serruya[a,1], Dhivakar Mani[a], Orly Marcu[a], Polina Stepensky[c], Yiska Weisblum[d], Esther Djian[d], Avraham Shaag[e], Shoshana Revel-Vilk[f,g], Iris Fried[f], Moshe Kotler[d], Alex Rouvinski[a], Dana Wolf[e], Orly Elpeleg[h,2], and Nayef Jarrous[a,2]

[a]Microbiology and Molecular Genetics, Institute of Medical Research Israel–Canada, The Hebrew University-Hadassah Medical School, 9112102 Jerusalem, Israel; [b]Brain Injury Clinic, Alyn Rehabilitation Hospital for Children, 91090 Jerusalem, Israel; [c]Pediatric Hematology-Oncology, Hadassah-Hebrew University Medical Center, 9112102 Jerusalem, Israel; [d]Department of Pathology and Immunology, The Lautenberg Center for Immunology and Cancer Research, The Hebrew University-Hadassah Medical School, 9112102 Jerusalem, Israel; [e]Microbiology and Infectious Diseases, Hadassah-Hebrew University Medical Center, 9112102 Jerusalem, Israel; [f]Pediatric Hematology/Oncology Unit, Shaare Zedek Medical Center, 9103102 Jerusalem, Israel; [g]The Hebrew University Hadassah Medical School, 9112102 Jerusalem, Israel; and [h]Department of Genetics, Hadassah-Hebrew University Medical Center, 9112102 Jerusalem, Israel

Edited by Thomas Shenk, Princeton University, Princeton, NJ, and approved July 30, 2020 (received for review May 26, 2020)

RNA polymerase (Pol) III has a noncanonical role of viral DNA sensing in the innate immune system. This polymerase transcribes viral genomes to produce RNAs that lead to induction of type I interferons (IFNs). However, the genetic and functional links of Pol III to innate immunity in humans remain largely unknown. Here, we describe a rare homozygous mutation (D40H) in the POLR3E gene, coding for a protein subunit of Pol III, in a child with recurrent and systemic viral infections and Langerhans cell histiocytosis. Fibroblasts derived from the patient exhibit impaired induction of type I IFN and increased susceptibility to human cytomegalovirus (HCMV) infection. Cultured cell lines infected with HCMV show induction of POLR3E expression. However, induction is not restricted to DNA virus, as sindbis virus, an RNA virus, enhances the expression of this protein. Likewise, foreign nonviral DNA elevates the steady-state level of POLR3E and elicits promoter-dependent and -independent transcription by Pol III. Remarkably, the molecular mechanism underlying the D40H mutation of POLR3E involves the assembly of defective initiation complexes of Pol III. Our study links mutated POLR3E and Pol III to an innate immune deficiency state in humans.

RNA polymerase III | innate immunity | cytomegalovirus | POLR3E | transcription

RNA polymerase (Pol) III primarily transcribes small noncoding RNAs, such as 5S rRNA and tRNA, which are implicated in essential biological processes in the cell (1–9). This polymerase is recruited to target genes by transcription factors that facilitate initiation and reinitiation of transcription (1–3, 9). Pol III is composed of 17 distinct protein subunits, some of which form specialized subcomplexes, i.e., RPC4/RPC5 (POLR3E), RPC8/RPC9, and RPC3/RPC6/RPC7 (10, 11). The first subcomplex is close to the polymerase active center, enables open promoter complex formation, and facilitates termination and reinitiation (12–14), whereas the last subcomplex consists of three specific subunits aiding in accurate initiation (11). Genes coding for protein subunits of Pol III, such as those of POLR3A, POLR3B, POLR1C, and POLR1D, are heterogeneously mutated in systemic morphological and neurological diseases, including Treacher Collins syndrome (15, 16) and demyelinating leukodystrophy (17–20). Part of these mutations leads to defects in the nuclear import, assembly, and chromatin occupancy of polymerase (19).

In addition to transcribing small noncoding RNA genes, Pol III is capable of transcribing synthetic DNA templates, such as poly [d(A-T)] and circular oligo-deoxyribonucleotides (coligos), in vitro and in cells (21–24). Transcription of poly [d(A-T)] templates by Pol III generates 5′-pppRNA transcripts that activate the cytoplasmic retinoic acid-inducible gene I (RIG-I) for downstream activation of the IFN regulatory factor IRF3 and induction of type I interferons (IFNs) (25–29). The latter IFNs act as primary mediators of antiviral responses initiated by macrophages and dendritic cells (25–29). The above transcription capability seems to be relevant to sensing and transcribing genomes of DNA viruses, e.g., human cytomegalovirus (HCMV) and herpes simplex virus-1, and bacteria by a cytosolic form of Pol III in invaded cells (25, 26, 30–33). Additional DNA-sensing pathways that detect non-AT-rich DNA templates for downstream induction of IFNs, but without producing corresponding transcripts, coexist in mice and human cells (26, 34–36). Recent studies link heterozygous inborn errors in several protein subunits of Pol III, including POLR3A, POLR3C, and POLR3E, to acute infections of susceptible children by the varicella zoster virus (VZV) (37, 38). Leukocytes derived from some of these unrelated children exhibit defects in type I IFN production and virus replication (36). Here, we describe a rare homozygous mutation (D40H) in POLR3E in a child that experienced lethal infections by DNA and RNA viruses and Langerhans cell histiocytosis (LCH). Strikingly, this recessive mutation impairs induction of type I IFN in response to viral infection and reduces Pol III output owing to assembly of functionally defective initiation complexes.

Significance

The innate immune system constitutes the host defense frontline against viruses. This system comprises several interrelated signal transduction pathways, one of which implicates the viral DNA sensor RNA polymerase (Pol) III. However, the link of this polymerase to innate immunity in humans remains largely unknown. Here, we describe a homozygous mutation (D40H) in the POLR3E gene, coding for a protein subunit of Pol III, in a child with disseminated viral infections and Langerhans cell histiocytosis. This mutation is related to diminished interferon induction and increased cell susceptibility to infection by cytomegalovirus. Strikingly, the D40H mutation leads to formation of functionally defective transcription complexes of Pol III. Our study links POLR3E and Pol III to an innate immundeficiency condition in humans.

Author contributions: A. Ramanathan, M.W., N.O., R.S., O.M., P.S., Y.W., A.S., M.K., A. Rouvinski, D.W., O.E., and N.J. designed research; A. Ramanathan, N.O., R.S., D.M., O.M., Y.W., E.D., A.S., S.R.-V., and I.F. performed research; O.E. contributed new reagents/analytic tools; A. Ramanathan, M.W., N.O., R.S., O.M., P.S., A.S., M.K., A. Rouvinski, D.W., O.E., and N.J. analyzed data; M.W., O.E., and N.J. wrote the paper; and N.O. obtained the data in Figs. 4, S4, and 6.

The authors declare no competing interest.

This article is a PNAS Direct Submission.

[1]A. Ramanathan, M.W., N.O., and R.S. contributed equally to this work.

[2]To whom correspondence may be addressed. Email: michaelweintraub1958@gmail.com, elpeleg@hadassah.org.il, or nayefj@ekmd.huji.ac.il.

This article contains supporting information online at https://www.pnas.org/lookup/suppl/doi:10.1073/pnas.2009947117/-/DCSupplemental.

First published August 25, 2020.

Results

A Mutation in the POLR3E Gene Is Identified in a Child with Systemic Viral Infections and Langerhans Cell Histiocytosis. A 1-y-old female, the third born to consanguineous parents, was suspected of having an innate immune deficiency owing to recurrent systemic viral infections and LCH (*SI Appendix*, Table S1). A search for common homozygous regions in the DNA of the patient using a single nucleotide polymorphism (SNP) array (39) identified nine genomic regions (*SI Appendix*, Table S2) that spanned ∼120 Mb and encompassed hundreds of protein-coding genes. These regions were not shared by the two unaffected sibs of the patient. In parallel, whole exome sequencing of the patient's DNA was performed and analyzed, as previously described (40). Variant filtering included removing those that were heterozygous, synonymous, low covered (less than ×7), off target, and those present at 0.1% in the Genome Aggregation Database (gnomAD) (https://gnomad.broadinstitute.org/) or in-house database dbSNP. Thirty variants passed this process, but only five of them resided within the linked regions and only two were predicted pathogenic by Mutation Taster software (41). The variants were chr16: 22319499 G > C, p.Asp40His (D40H) in the *POLR3E* gene (rs200525630) and chr2: 190328455 G > A, p.Ala325Thr in the *WDR75* gene (rs149368656, minor allele frequency 0.04%) (*SI Appendix*, Table S2). The WDR75 mutation was carried by 135 of 138,452 healthy individuals subjected to exome sequencing analyses available at the gnomAD, with no homozygous state reported. Therefore, we focused on the *POLR3E* gene, which has a recessive D40H mutation segregated with the disease in the family (Fig. 1*A*) and codes for a protein subunit of Pol III shown to be implicated in the innate immune system (25, 26, 36). Of note, a single case of homozygous D40H mutation was found in the gnomAD, whereas the heterozygous state was carried by 49 out of 138,089 healthy individuals. Hence, the homozygous D40H mutation describes a rare variant of POLR3E. Comparative structural modeling analyses using the Rosetta software suite (42) and the known three-dimensional (3D) structures of the yeast POLR3E (RPC5) and Pol III (8, 43), delineated the D40H mutation in the flexible domain of human POLR3E (Fig. 1*B*) and exterior region of the polymerase bound to DNA (Fig. 1*C*).

Patient's Fibroblasts Exhibit a Deficient Antiviral Response. The recurrent viral infections described above prompted us to examine if the D40H mutation of POLR3E affects type I IFN induction in response to cell infection by HCMV (25, 26). Thus, cultured primary fibroblasts derived from the patient and control individuals were subjected to infection with HCMV and expression of the IFN-β mRNA was followed by quantitative real-time PCR (*Materials and Methods*). An approximately fourfold decrease in IFN-β mRNA levels was detected in the patient's cells on the

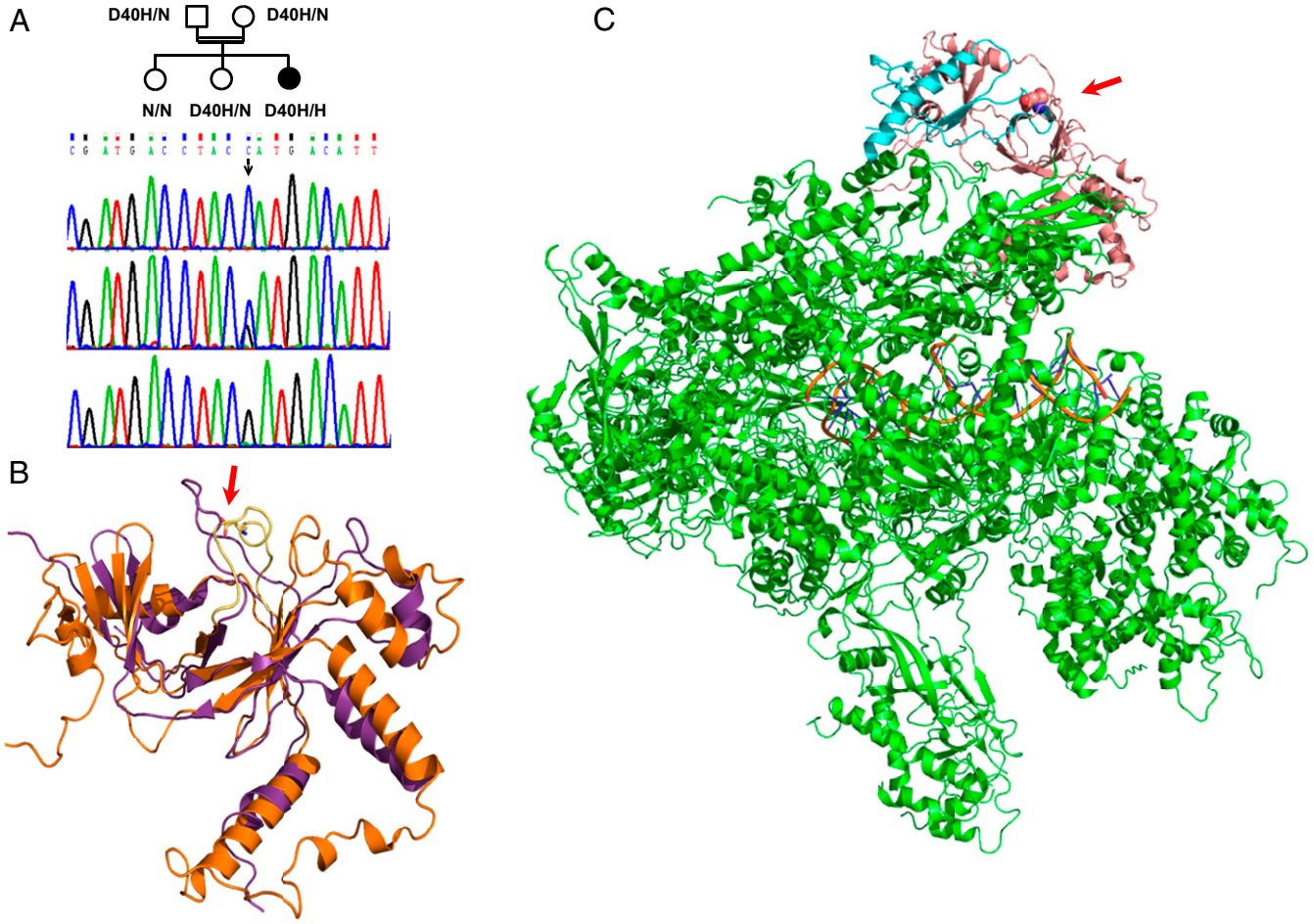

Fig. 1. The D40H mutation inheritance and its position in POLR3E and Pol III. (*A*) Segregation of the D40H mutation in the POLR3E gene in the patient's family pedigree. The genomic sequence around the mutation site (arrow) in the patient (*Upper*; G-to-C substitution), an obligatory carrier (*Middle*), and control (*Lower*) are shown. (*B*) Structural model of POLR3E (RPC5) was generated by the Rosetta software suite for protein structure prediction. The structure (in orange) is superimposed onto the solved structure of the yeast counterpart RPC5 (purple) (43). Arrow points to the D40H mutation, which seems to lie in a structurally flexible region. (*C*) Structure of the entire complex of yeast Pol III (green) bound to DNA (orange) (8, 43), but the RPC5 subunit was replaced with that of the human counterpart, POLR3E (pink). POLR3E interacts with RPC4 (blue). Arrow points to the D40H mutation.

first and fifth day of infection, when compared with those measured in the control fibroblasts (Fig. 2 *A* and *B*; $P = 0.038$). By contrast, an approximately twofold increase in the viral immediate early 1 (IE1) mRNA level was evident in the patient's cells (Fig. 2 *A* and *B*; $P = 0.0035$). These results point to impairment of IFN-β mRNA induction and increased susceptibility of cells to HCMV infection. Comparable deficiency in IFN-β production and enhanced vulnerability to VZV infection were reported in peripheral blood mononuclear cells (PBMCs) obtained from children with inborn mutations in the subunits POLR3A and POLR3E (36).

The compromised response of IFN expression described above was not due to a general failure of patient's cells to respond to external cues. Thus, dendritic cells (DCs) externally treated with lipopolysaccharide (LPS) or synthetic dsRNA (poly I:C) displayed normal induction of expression of HLA-DR and costimulatory molecule CD86 (*Materials and Methods*), as well as typical development of immature DCs (iDCs) (*SI Appendix*, Figs. S1 and S2). Therefore, the patient's DCs have functional TLR3 and TLR4 signal transduction pathways of the innate immune system (29).

Viral Infection Induces the Expression of POLRE3 in Cultured Cell Lines. Because of shortage in the patient's cells, we used human cell lines to assess the relationship between POLR3E/Pol III and viral infections. We found that infection of the retinal pigment epithelial cell line ARPE-19 by HCMV led to an approximately threefold increase in the steady-state level of POLR3E (Fig. 3*A*, ~80 kDa) (*Materials and Methods*). A comparable increase in POLR3E was observed in HEK293 cells infected for 16 h with sindbis virus (Fig. 4*A*, lanes 8 vs. 10; Fig. 4*B* and *SI Appendix*, Fig. S3, lanes 8 vs. 10), a positive ssRNA virus with a 3′-sequence enriched with AU (44). By contrast, POLR3E expression decreased in cells infected with a vesicular stomatitis virus (VSV), when compared with that measured in uninfected cells (Fig. 4*A*, lanes 6 vs. 10; Fig. 4*B*; *SI Appendix*, Fig. S3, lanes 9 vs. 10), and remained largely unaltered after infection with vaccinia virus and HIV-1 (Fig. 4, lanes 7 and 9 vs. 10; Fig. 4*B*; *SI Appendix*, Fig. S3, lanes 6 and 7 vs. 10) (*Materials and Methods*). VSV, a negative ssRNA virus, has been reported to activate RIG-I, but not Pol III, in priming an innate immune response in murine glial cells (31). An approximately fourfold increase in the expression of Rpp25, a protein subunit of the ribonucleoprotein RNase P shown to be associated with Pol III in initiation complexes (45), was measured in cells infected for 16 h with sindbis virus (Fig. 4*A*, lanes 8 vs. 10; Fig. 4*C*; *SI Appendix*, Fig. S3, lanes 8 vs. 10). All viral infections described above were performed at low multiplicity of infection (MOI = 0.1 to 0.2; *Materials and Methods*), thereby keeping the cells viable throughout the experiment (*SI Appendix*, Fig. S4).

The results demonstrate that POLR3E expression is induced by DNA and RNA viruses in infected cells. However, induction is not confined to this protein subunit of Pol III (see below).

Plasmid DNA Induces Expression of POLR3E. Induction of POLR3E expression by different viruses as described above raised the question of whether foreign nonviral DNA can induce the expression of this protein. Remarkably, cells that were transfected with increasing amounts of plasmid DNA, pBluescript II (SK), exhibited elevated steady-state levels of POLR3E (Fig. 5*A*, lanes 1 to 4 and Fig. 4*F*). Expression of the subunits RPC6 and RPC7 slightly increased in the presence of low amounts of plasmid DNA (Fig. 5 *C*, *D*, *H*, and *I*). By contrast, the steady-state levels of GAPDH remained unchanged (Fig. 5 *E* and *J*). The above increase in POLR3E expression was independent of the transfection reagent or plasmid backbone (see below). Strikingly, Pol III capability in transcription increased by several folds (approximately sixfold), as manifested in the elevated transcription of 5S rRNA gene in whole S20 extracts prepared from the transfected cells (Fig. 5*B*, lanes 1 vs. 2 to 4; Fig. 5*G*) (*Materials and Methods*) (45, 46). Transcription peaked at a subconcentration of the plasmid DNA (Fig. 5*B*, lanes 3 vs. 4) and partially coincided with the induced expression of POLR3E (Fig. 5*A*, lanes 3 vs. 4).

The results reveal that foreign DNA induces the expression of POLR3E and activates Pol III transcription (see below). These findings are consistent with previous studies demonstrating that viral infections elicit Pol III activity, as judged from inhibition assays using chemical inhibitors of the polymerase (26, 27, 37).

Activation of Pol III Transcription Is Precluded by Ectopic Expression of a D40H Mutant POLR3E. The above transcription system was utilized to check if exogenous expression of a D40H mutant POLR3E affects activation of Pol III. Thus, HEK293 cells were transiently transfected with expression vector carrying a cDNA coding for a D40H mutant or wild-type POLR3E (Fig. 6; *Materials and Methods*). Low and high efficiencies of transfection (Fig. 6*A*, lanes 3 to 6 vs. 7 to 10, respectively), as assessed by visualization of coexpressed GFP using fluorescent microscopy (*Materials and Methods*), were carried out, and S20 extracts were prepared at 24 and 42 h after transfection. A ~10-fold increase in transcription of 5S rRNA gene was measured in extracts of cells transfected with an empty vector, when compared with that obtained in extracts of cells mock transfected without plasmid (Fig. 6*A*, lanes 3 vs. 4 and 7 vs. 8; *SI Appendix*, Fig. S5*A*). Remarkably, ectopic expression of the wild-type POLR3E had partial or no effect on transcription of the 5S rRNA gene (Fig. 6*A*, lanes 4 vs. 5 and 8 vs. 9; *SI Appendix*, Fig. S5*A*), whereas that of the mutant protein reduced the increase in transcription (Fig. 6*A*, lanes 4 vs. 6 and 8 vs. 10; *SI Appendix*, Fig. S5*A*). In fact, expression of the mutant protein brought down transcription to

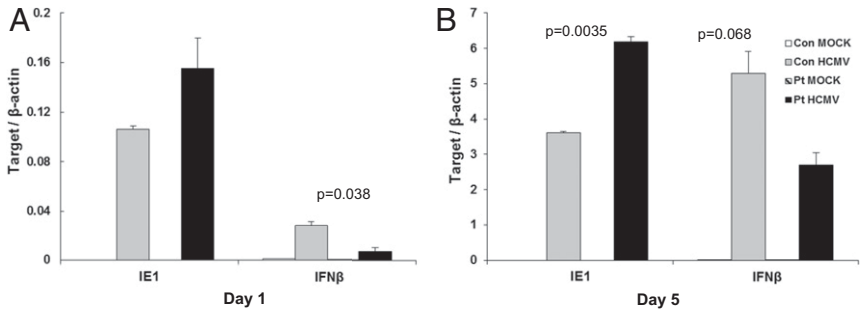

Fig. 2. Patient's fibroblasts exhibit impaired induction of the IFN-β gene and enhanced susceptibility to infection with HCMV. Cultured skin fibroblast from the patient and control individual (Pt, patient; Con, control) were infected with HCMV strain TB40/E. Total RNA was extracted from cells at day 1 (*A*) and day 5 (*B*) after virus infection, and IFN-β mRNA and viral IE mRNA levels were analyzed by quantitative RT-PCR and normalized to the β-actin mRNA. The results represent the mean values of five independent replicate wells. Error bars represent SD.

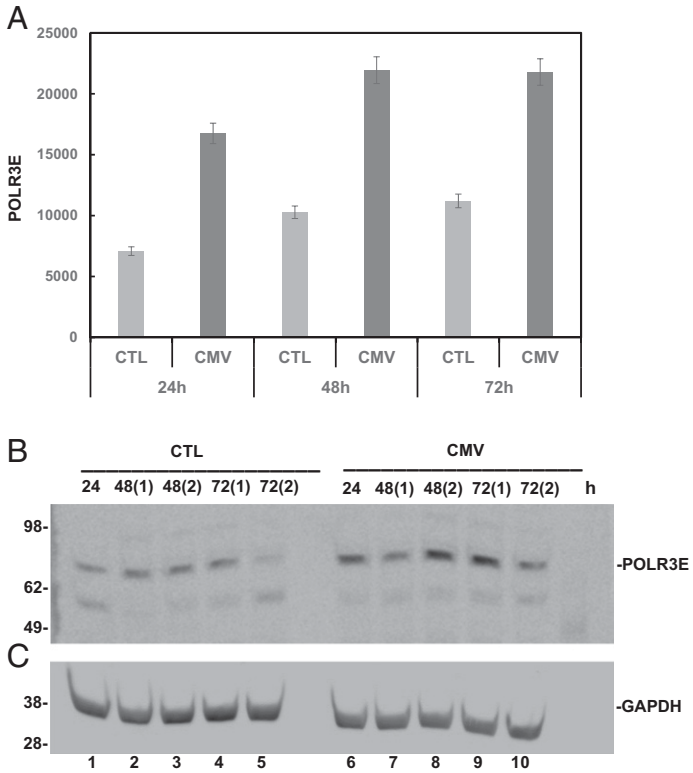

Fig. 3. Infection of cells with HCMV induces expression of POLR3E. (*A*) Cultured ARPE-19 cells were infected with HCMV for the indicated time points. Whole cell extracts (S20) were then prepared and subjected to Western blot analysis using antibodies against POLR3E and GAPDH (*Materials and Methods*). The signal intensities of the POLR3E bands, normalized to those of GAPDH, were quantified and plotted. The *y* axis denotes arbitrary units. Similar results were obtained in three independent experiments. Error bars represent SD. (*B* and *C*) Western blot analysis of the POLR3E (~80 kDa) and GAPDH (~38 kDa) that were plotted in *A*.

low levels almost comparable to those obtained in the control cells that were mock transfected without plasmid (Fig. 6*A*, lanes 3 vs. 6 and 7 vs. 10; *SI Appendix*, Fig. S5*A*).

The above inhibitory effect of expression of the D40H mutant POLR3E on transcription was not limited to that of the 5S rRNA gene. Thus, a similar outcome was obtained with the use of a human $tRNA^{Arg}$ (UCU) gene (45), whose transcription was low in S20 extracts of cells expressing the mutant protein, but not the wild-type polypeptide (Fig. 6*D*, lanes 4 vs. 6 and 8 vs. 10; *SI Appendix*, Fig. S5*B*). Likewise, transcription of a synthetic coligo DNA template (Fig. 6*C*) was low in extracts derived from cells expressing the mutant protein (Fig. 6*B*, lanes 4 vs. 6 and 8 vs. 10; *Upper* band; *SI Appendix*, Fig. S5*C*), but high in those prepared from cells expressing the wild-type protein (Fig. 6*B*, lanes 4 vs. 5 and 8 vs. 9; *SI Appendix*, Fig. S5*C*). The promoter-independent transcription of coligo DNAs was shown to be primarily carried out by a cytoplasmic Pol III (23), a form apparently involved in sensing of DNA viruses (25, 26).

Expression of the D40H Mutant POLR3E Leads to Formation of Defective Initiation Complexes. The yeast homolog of POLR3E, C37, and its interacting partner C53 are implicated in promoter opening at initiation (13, 47, 48). Therefore, we asked if the above inhibitory effect of expression of the exogenous D40H mutant POLR3E on transcription (Fig. 7*A*, lanes 3 vs. 4) was due to formation of defective initiation complexes. To address this issue, initiation complexes were assembled on the $tRNA^{Arg}$ gene in extracts having mutant or wild-type proteins (Fig. 7 *B*, *Upper*), purified by velocity sedimentation in 15 to 40% glycerol gradients, and then examined for transcription (*Materials and Methods*) (45). Strikingly, initiation complexes that were assembled in the extract of cells expressing the mutant protein displayed low transcription, when compared with those of the control extract (Fig. 7*C* vs. Fig. 7*D*, F5–F15). Coimmunoprecipitation analysis using an antibody against the specific subunit RPC3 indicated that the content of POLR3E in the peak fractions enriched with active Pol III was less than that of the wild-type form (Fig. 7*E*, lanes 6 vs. 7). This difference was not due to low expression of the D40H mutant POLR3E in the cells. In fact, expression of the mutant protein in the cells was higher than that of the wild-type protein (Fig. 7*B*, lanes 3 vs. 4). Hence, the low transcription seen in extracts containing the D40H mutant POLR3E (Fig. 7*A*) was due to formation of functionally impaired initiation complexes, as compared to proficient complexes formed in the presence of the wild-type polypeptide. Furthermore, the impaired initiation complexes mainly sedimented in the upper fractions with a peak seen in fraction F5, when compared to those of the control complexes that peaked in fractions F9–F13 (Fig. 7*C* vs. Fig. 7*D*, F5–F15). Notably, coexpression of the wild-type and mutant POLR3E in transfected cells (Fig. 7*B*, lane 5 vs. 3 and 4) did not rescue transcription (Fig. 7*A*, lanes 5 vs. 3 and 4), possibly due to the transient expression of these proteins or dominant-negative effect of the mutant form.

The above results uncover that the molecular mechanism underlying the inhibitory effect of the D40H mutation of POLR3E on transcription involves the assembly of structurally and functionally defective initiation complexes of Pol III.

Discussion

We have described a rare recessive mutation in POLR3E in a child with lethal viral infections and LCH. This D40H mutation is linked to increased susceptibility of the patient's cells to HCMV infection and impaired induction of type I IFN. Even

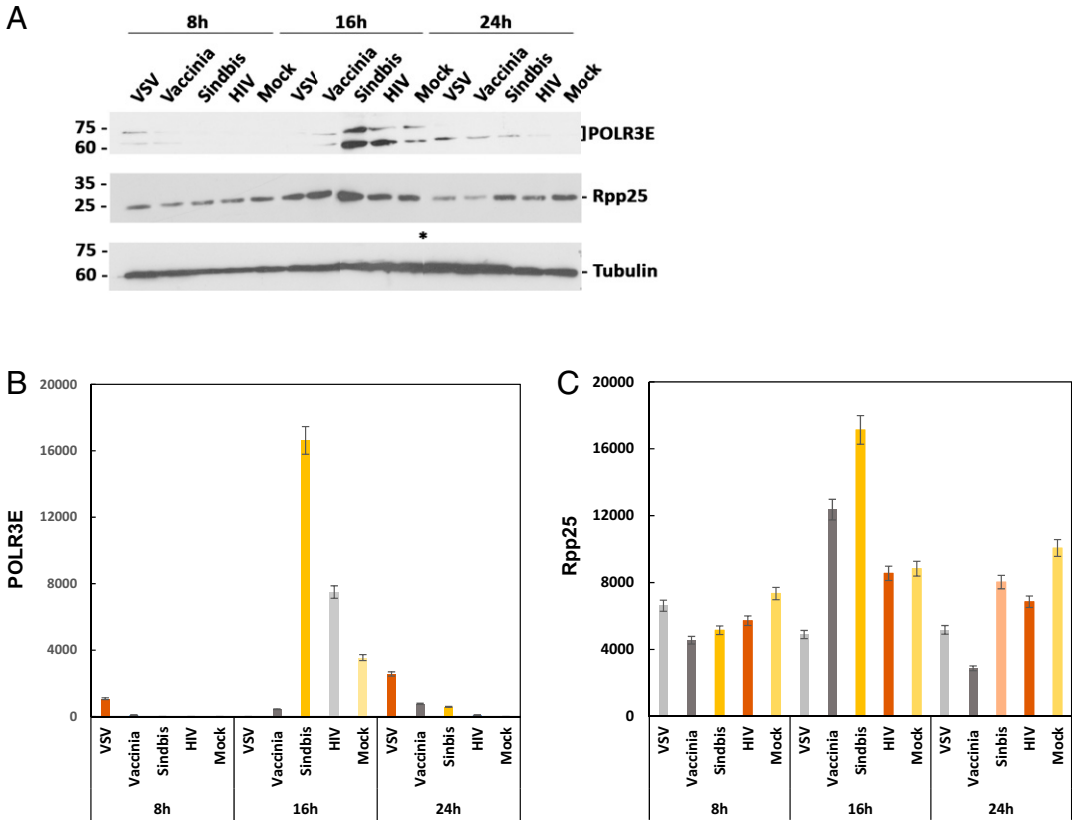

Fig. 4. Expression of POLR3E in HEK293 cells infected by different viruses. (*A*) HEK293 cells were infected with the indicated viruses (*Materials and Methods*) for the specified time points. Whole cell extracts (S20) were then prepared and subjected to Western blot analysis using antibodies against POLR3E, Rpp25, and β-tubulin. The positions of protein size markers (in kilodaltons) are depicted. A composite of two minigels (lanes 1 to 7 and 8 to 15; asterisk) of the same electrophoresis analysis is shown. (*B* and *C*) The signal intensities of the POLR3E and Rpp25 (25 kDa) bands seen in *A*, and normalized to those of β-tubulin, were plotted. The *y* axis represents arbitrary units.

though we could not find other patients to establish the genetic inheritance of the rare D40H mutation and its link to the severe clinical manifestations (*SI Appendix*, Table S1), we did show that exogenous expression of a D40H mutant POLR3E in cells leads to a marked reduction in activation of Pol III transcription by foreign DNA, owing to the assembly of malfunctioning transcription complexes of the polymerase. Moreover, we demonstrate that expression of POLR3E, and possibly other protein subunits, increases in response to the presence of viral and nonviral nucleic acids in cells, while high expression of POLR3E brings to a striking activation of Pol III transcription. The observed accompanying fulminant infections of our patient with RNA viruses, such as respiratory syncytial virus, human metapneumovirus, and parainfluenza 3 (*SI Appendix*, Table S1) remain unexplained, but failure to respond to opportunistic or primary infections with these viruses due to mutated POLR3E should be taken into consideration. In this respect, we demonstrate that POLR3E expression is induced in cells infected with sindbis virus, a positive ssRNA virus with a genomic 3′-terminal noncoding sequence enriched with AU (~90%) (44). Therefore, our study unveils that select DNA and RNA viruses induce the expression of POLR3E.

Several DNA-sensing pathways have been reported to exist in the human and mouse innate immune systems (25, 26, 34). One pathway involves AT-rich DNA sensing and transcription by Pol III for downstream activation of RIG-I and production of type I IFNs, whereas a second pathway includes sensing of non-AT-rich DNA, but without transcribing the DNA (25, 26). As to the latter pathway, it has been demonstrated that induction of type I IFNs is achievable in cells transfected with poly [d(G-C)], PCR DNA fragments, and plasmid DNA without being transcribed by Pol III (25, 26, 34). In this study, we demonstrate induction of POLR3E expression in response to transfection of cells with circular or linear plasmid DNA (e.g., pBluescript, pcDNA3, and pEGFP-C1) and that this induction is associated with activation of Pol III transcription, thereby supporting a role of POLR3E and Pol III in responding to nonviral DNA.

Whole exome sequencing analyses reveal that the homozygous D40H mutation of POLR3E occurs in an apparently healthy 1-y-old child. Accordingly, this case raises the question of why our child patient developed recurrent, lethal infections by viruses (*SI Appendix*, Table S1). A predisposition variation to virus infections is one possibility. A predisposition variation has been described for VZV infection severity in healthy children carrying heterozygous inborn errors in the subunits POLR3A, POLR3C, and POLR3E (36–38, 49). Another possibility that could have contributed to the lethal viral infections in our patient is a second genetic hit, for instance, the occurrence of genetic changes in nonexonic sequences that were not covered by the genetic techniques utilized in this study. Nonetheless, the direct inhibitory effect of the expression of exogenous D40H mutant POLR3E on transcription and formation of aberrant initiation complex (Figs. 6 and 7) argue against such a possibility. A third option is the concurrent LCH, from which our patient suffered along with systemic viral infections. LCH has a wide clinical spectrum ranging from isolated bone or skin lesions that may regress without treatment to life-threatening multiorgan lesions (50–52). Current models relate the pathogenesis of LCH to the

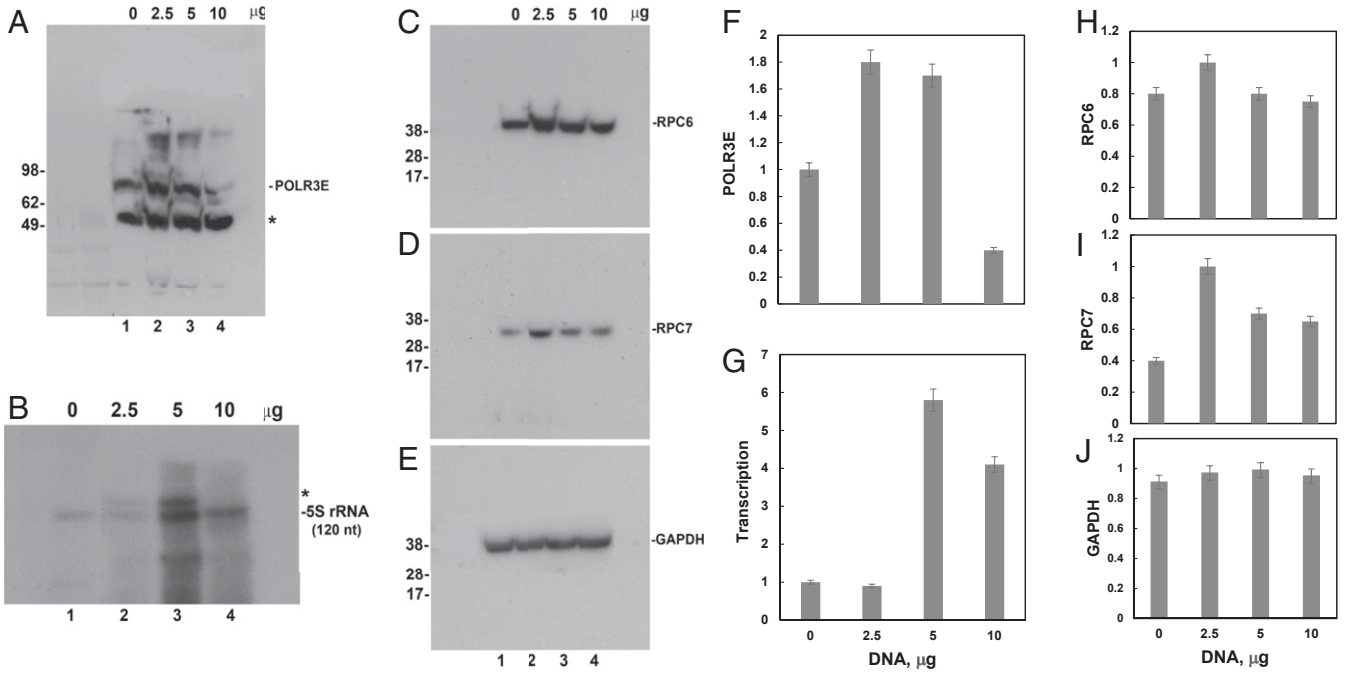

Fig. 5. Expression of POLR3E and Pol III activity are enhanced in cells transfected with plasmid DNA. (*A–E*) HEK293 cells were transfected with increasing amounts of circular plasmid DNA, pBluescript (SK). Whole cell extracts were prepared at 42 h and subjected to Western blot analysis using antibodies against POLR3E, RPC6, RPC7, and GAPDH, as indicated. Protein size markers (in kilodaltons) are shown. Asterisk points to nonspecific band or short POLR3E form. In *B*, extracts were also assayed for 5S rRNA gene transcription (*Materials and Methods*) and the position of the ^{32}P-labeled 5S rRNA in 10% denaturing polyacrylamide/7 M urea gel is indicated. Asterisk points to a nonspecific RNA or product of inaccurate initiation or termination of 5S rRNA gene transcription. (*F–J*) The relative signal intensities of POLR3E, RPC6, and RPC7 described above were normalized to those of GAPDH and plotted. The signal intensities of the labeled 5S rRNA band (120 nt) described above are presented in *G*.

proliferation of DCs due to a clonal neoplasm or an anomalous immune response (53). In the former model, LCH is classified as an inflammatory myeloid neoplasm predominantly caused by mutations in the MEK/ERK pathway, frequently affecting BRAF and MAP2K1 (50, 53–56). A role of viral infections in LCH pathogenesis has been previously considered, but without having definitive conclusions (57, 58). LCH patients have not been reported to display innate immunodeficiency or defined susceptibility to infectious agents (59). Therefore, our study supports the option that the LCH had progressed to a life-threatening stage in our patient due to recurrent primary or opportunistic viral infections and persistent activation of DCs taking place under an innate immunodeficiency condition. The latter condition is apparently linked to the D40H-mutated POLR3E and Pol III unable to mount an antiviral immune response via type I IFN induction.

Our study shows that the molecular mechanism underlying the inhibitory effect of the D40H mutation of POLR3E on Pol III transcription involves the generation of functionally defective initiation complexes, which could be gently purified and assessed by velocity sedimentation analysis in glycerol gradients. This functional defect is not linked to a lack in the expression of the mutant POLR3E in transfected cells. On the contrary, the steady-state level of the mutant protein is higher than that of the wild-type form (Fig. 7 *A*, *Lower*). Instead, the position of POLR3E in the Pol III complex (Fig. 1*C*) and the close proximity of the mutation to the interacting partner RPC4 (Fig. 1*C*, arrow) support the molecular interpretation that the replacement of the negatively charged aspartic acid with histidine in POLR3E alters the assembly of Pol III in stably proficient initiation complexes. Clinically related mutations in the interacting protein subunits POLR1C and POLR1D have been shown to destabilize yeast Pol III complex integrity (16). Therefore, solving the structure of Pol III carrying the D40H-mutated POLR3E, or other pathogenic mutations (19, 20, 36–38, 49, 60), could be of general interest in understanding the mode of action of this sensor polymerase in infectious and genetic diseases in the future.

Materials and Methods

Cells, Virus Infection, and Transfection. Primary foreskin fibroblasts were used to propagate HCMV strain TB40/E, as previously described (61). Virus titers of the cleared supernatants were determined by the standard plaque assay on human foreskin fibroblasts. For virus infection, skin fibroblasts from the patient and controls were grown in Dulbecco's modified Eagle's medium (DMEM) supplemented with 10% fetal bovine serum, 2 mM glutamine, 100 IU/mL penicillin, 100 μg/mL streptomycin (Biological Industries) and 0.25 μg/mL fungizone (Invitrogen), and at ~80% confluence cells were infected with HCMV strain TB40/E at a MOI of 0.1 to 0.2.

The Vero adherent cell line was grown as a subconfluent monolayer in DMEM and the T lymphocyte cell line Sup T1, provided by the NIH Reagent Program (Division of AIDS, National Institute of Allergy and Infectious Diseases, NIH), was grown in RPMI medium 1640 (Biological Industries). Vaccinia (Lister), VSV (Indiana), and sindbis virus were propagated and titered by the classical plaque assay on Vero cells. HIV-1 was generated by transfection of HEK293 cells with pSVC21 plasmid containing full-length HIV-1HXB2 viral DNA. Titration of HIV-1 was carried out by the multinuclear activation of a galactosidase indicator (MAGI) assay.

Adherent HeLa S3 and HEK293 cells were grown in 92 × 17 mm-style Petri dishes in DMEM supplemented with 5% fetal bovine serum, streptomycin (100 μg/mL), penicillin (100 units/mL), and nystatin (12.5 units/mL). Cells were incubated in 5% CO_2 at 37 °C. ARPE-19 cells were grown in 92 × 17 mm-style Petri dishes in DMEM/F12 supplemented with 1% L-glutamine, 1% penicillin/streptomycin/nystatin, and 10% fetal bovine serum. For viral infections, HEK293 at ~80% confluence were infected with the aforementioned vaccinia virus, VSV, sindbis virus, and HIV-1 at MOI of 0.1 to 0.2.

For cell transfection, HEK293 cells at 30 to 50% confluence were transfected with an expression vector carrying wild-type or D40H-mutant POLR3E cDNA (10 to 15 μg) in 10 mL medium using the polyethyleneimine (PEI) or calcium phosphate method (45, 46). Optimal DNA:PEI ratio was 1:3. The

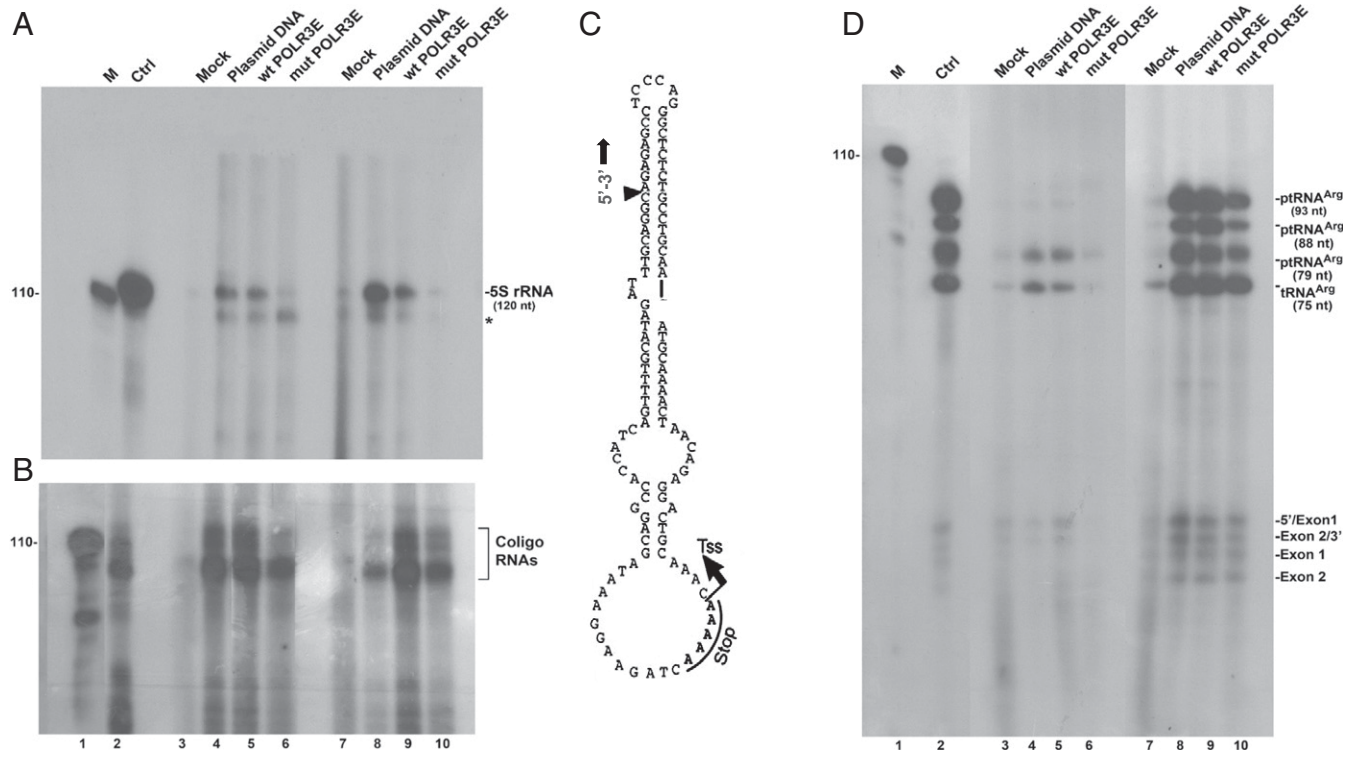

Fig. 6. Exogenous expression of a D40H mutant POLR3E precludes promoter-dependent and -independent transcription of Pol III. HEK293 cells were transfected with expression vector encoding wild-type POLR3E or D40H mutant POLR3E, as shown. As controls, cells were mock transfected or transfected with pBluescript alone for 42 h. Two sets of whole extracts (S20) seen in lanes 3 to 6 and lanes 7 to 10 were prepared and transcription of human 5S rRNA gene (*A*), coligo 19anbBR2 (*B*), and $tRNA^{Arg}$ gene (*D*) was evaluated (*Materials and Methods*), as previously described (45). The positions of the precursors, mature and cleaved exons of $tRNA^{Arg}$, are denoted. In *B*, the major coligo RNA transcripts are demarcated by a bracket. In all panels, lane 2 represents transcription reactions in control large-scale HeLa cell extracts. Lane 1 shows 110-nt RNA size marker. To fit the running order of all gels, a composite of three parts of gel autoradiogram is seen in *D*. In *A*, the asterisk points to nonspecific RNA band. (*C*) Sequence and predicted secondary structure of the coligo 19anbBR2 DNA (23) used as a template for promoter-independent transcription of Pol III seen in *B*. The coligo is made of two annealing synthetic deoxyoligonucleotides. Arrowhead denotes the site of the coligo circularization, a ligation reaction executed in the extract via an unknown mechanism (23). Small arrow points to DNA direction. The start (Tss) and termination (Stop) sites of transcription are indicated.

expression vector harbors a separate GFP reporter gene for assessment of transfection efficiency by fluorescent microscopy and Western blot analysis. After transfection, cells were harvested and extracts were prepared and tested for transcription of human 5S rRNA and $tRNA^{Arg}$ genes, as previously described (45, 46, 62). Whole cell extracts (S20) with protein concentrations of 10 to 15 mg/mL were used (45, 46). For promoter-independent initiation, the circularized coligo 19anbBR2 DNA was added as a template for transcription by Pol III (23). This coligo DNA is made of two annealing synthetic deoxyoligonucleotides and mainly transcribed by cytoplasmic Pol III (24).

Dendritic Cells, Differentiation, and Activation. For the generation of monocyte-derived dendritic cells, immature monocyte-derived dendritic cells (iDCs) were generated from the $CD14^+$ selected fraction of PBMCs isolated from deidentified fresh peripheral blood of the patient and nonrelated healthy controls. For iDCs, PBMCs were isolated using Ficoll-Paque (Amersham Pharmacia Biotech) and anti-CD14 magnetic beads in order to isolate monocytes from PBMCs according to the manufacturer's instructions (Becton Dickinson). iDCs were placed in wells at a concentration of 1.25×10^6/1.5 mL. Culture medium consisted of RPMI 1640 with 1% L-glutamine, 1% penicillin/streptomycin (Biological Industries), 1% autologous human plasma, and recombinant human cytokines GM-CSF and IL-4 (R&D Systems or PeproTech). Every 2 d, 0.15 mL was removed and 0.25 mL of media containing plasma, IL-4, and GM-CSF, 500 U/mL, was added. On day 6, iDCs were harvested, washed, and counted.

For activation of iDCs, the 6-d cultured cells described above were collected, washed, and replated in 96-well plates at a concentration of 1×10^6 cells/mL. LPS and poly I:C (Sigma-Aldrich) were added to final concentrations of 10 ng/mL and 50 μg/mL, respectively. After 24 h, cells were collected, washed, and immunostained for HLA-DR and CD86 markers using mouse anti-human HLA-DR-PE and mouse CD86-PE and isotype control (Biolegend) and for DC-sign using a mouse anti-human DC-sign-fluorescein isothiocyanate (FITC) (R&D Systems). Cells were analyzed by a FACS Calibur flow cytometer (BD).

RNA Quantification. RNA was extracted from infected skin fibroblast cultures using the NucleoSpin RNA II Kit (Macherey-Nagel), according to the manufacturer's instructions. The purified RNA samples were subjected to reverse transcription using GoScript (Promega), followed by quantitative real-time PCR of the immediate early 1 (IE1) HCMV mRNA, as previously specified (61). Quantitative real-time PCR of IFN-β mRNA was carried out using primers and probe designed by the Primer 3 program. The viral and IFN-β mRNA copy numbers were normalized to that of the housekeeping β-actin mRNA (61). A P value less ≤ 0.05 is statistically significant.

Relative changes in POLR3E mRNA were calculated using quantitative real-time PCR analysis. Total RNA was isolated from the patient and three healthy control fibroblasts. Samples of 15 ng of RNA were used as templates for cDNA preparation using random primers (Promega, A3802). RT-PCR was performed using Sybr green assay (Roche). The POLR3E mRNA was measured at three different nucleotide positions: the boundary of exons: 4 to 5, 12 to 13, and 17 to 18. POLR3Eex4 to 5 (108 bp) forward primer: 5′-GGAGCAGATTGCGCTGAA-3′, reverse primer: 5′-TTACTGGTGGTCTGGGAAGA-3′. POLR3Eex12 to 13 (77 bp) forward primer: 5′-CCAGAAGGTGGCGATGTT-3′, reverse primer: 5′-GGCTGGACGAGTCCTTG-3′. POLR3Eex 17 to 18 (100 bp) forward primer: 5′-CCGGTTGCAAGCAGATACT-3′, reverse primer: 5′-TCACTCATGTCTCCAGACTCC-3′. Delta Ct (2-ΔΔct) values were calculated using the GAPDH gene as a reference. GAPDH exons 2 to 3 (98 bp) forward primer: 5′-ATGGGGAAGGTGAAGGTCGG-3′, reverse primer: 5′-TGACGGTGCCATGGAATTTG-3′.

In Vitro Transcription and Purification of Initiation Complexes of Pol III. Transcription reactions were performed for 1 to 3 h of incubation at 30 °C in a total volume of 25 μL that contained 15 μL of whole cell extract (S20), 1× transcription buffer, nucleoside triphosphates (NTPs), 10 μCi of [α-^{32}P]-UTP

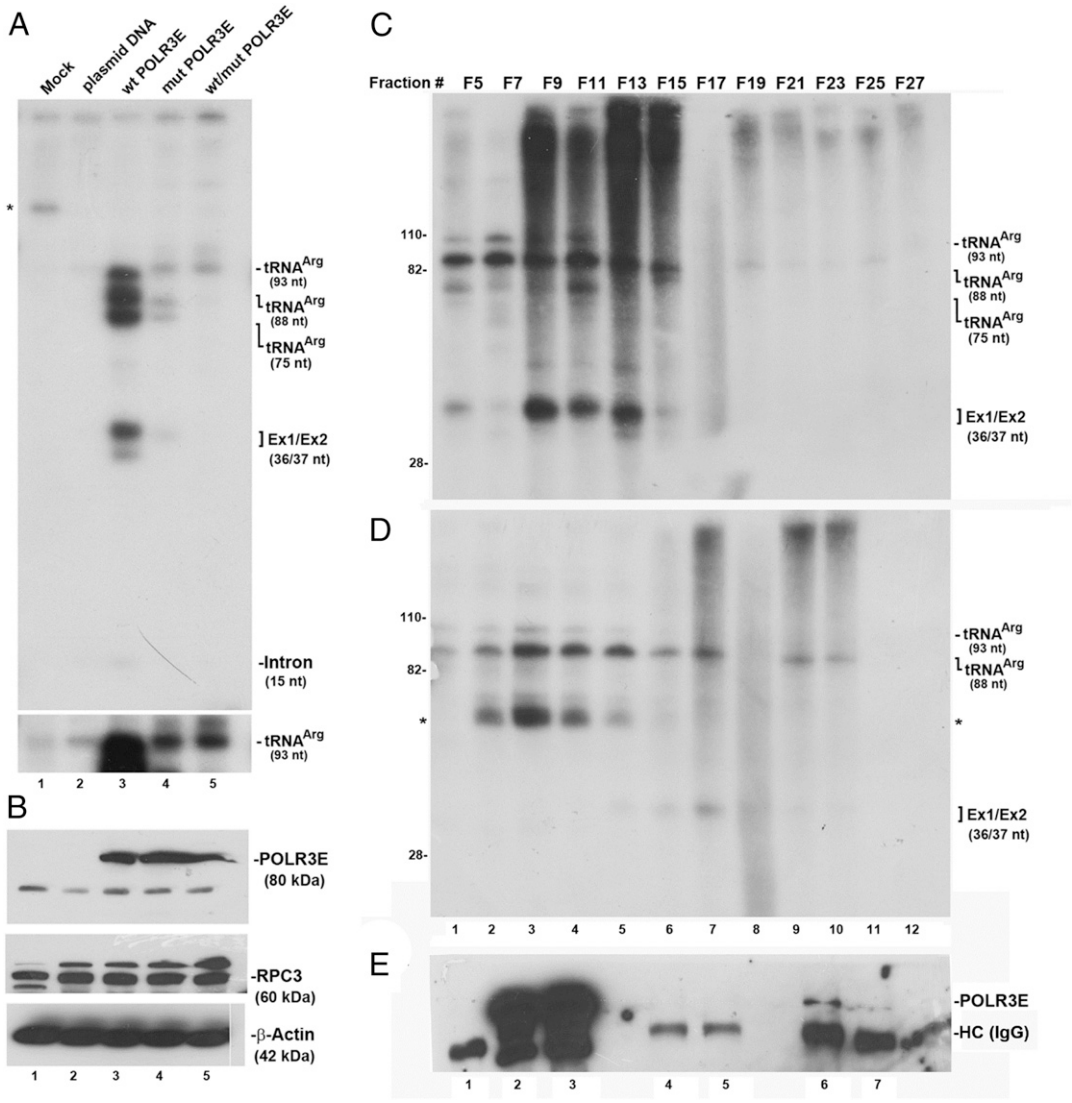

Fig. 7. Formation of impaired initiation complexes of Pol III in extracts derived from cells expressing a D40H mutant POLR3E. (*A*) HEK293 cells were transfected with eukaryotic vector expressing wild-type POLR3E (lane 3), D40H mutant POLR3E (lane 4), or both (lane 5). As controls, cells were treated with the transfection reagent PEI (lane 1) or PEI with pBluescript (SK) (lane 2). After 48 h, cells were harvested, whole S20 extracts were prepared and subjected to in vitro transcription of human $tRNA^{Arg}$ gene, as described in Fig. 6*D*. The positions of the precursors, mature and cleaved exons of $tRNA^{Arg}$ in a 10% sequencing gel are indicated. Asterisk points to nonspecific band. (*B*) Western blot analysis of the S20 extracts described in *A* using antibody against POLR3E, RPC3, and β-actin. (*C* and *D*) S20 extracts from transfected cells expressing wild-type POLR3E, mutant POLR3E, or both, as shown in *A*, were used for assembly of initiation complexes on a human $tRNA^{Arg}$ gene, as previously described (45). The resulted initiation complexes were then separated by velocity sedimentation in 15 to 40% glycerol gradients by ultracentrifugation (*Materials and Methods*). Fractions were collected from the top of each gradient and immediately were tested for $tRNA^{Arg}$ gene transcription for 3 h. Labeled RNA was then extracted and analyzed by electrophoresis in a 10% sequencing gel. The positions of the precursors, mature and cleaved exons of $tRNA^{Arg}$, are specified. The positions of RNA size markers, whose intrusive labels were erased, are shown on the *Left*. Asterisk in *D* points to nonspecific band. (*E*) Coimmunoprecipitation of wild-type and mutant POLR3E with the specific subunit RPC3 of Pol III. Fractions F5–F15 with peak transcription activities seen in *C* and *D* were combined and subjected to coimmunoprecipitation analysis using an antibody against RPC3. The immunoprecipitates were then subjected to Western blotting using an antibody against POLR3E (lanes 6 and 7). The position of the POLR3E is shown. As controls, the same F5–F15 fractions containing wild-type and mutant POLR3E (lanes 2 and 3) were analyzed by an IgG antibody (lanes 4 and 5). For spotting the heavy chain of IgG, a sample of IgG antibody alone was blotted (lane 1).

(3,000 Ci/mmol; PerkinElmer), and 0.25 to 0.5 μg of plasmid DNA carrying tRNA or 5S rRNA gene (45, 46) or circularized coligo 19anbBR2 DNA (23). The reaction mixtures were then diluted 1:1 with H_2O, passed through G-50 columns, diluted to 0.25 mL with 1× digestion buffer, and digested with 120 μg/mL Proteinase K for 30 min at 37 °C. Labeled RNAs were recovered by phenol:chloroform:isoamyl alcohol extraction followed by ethanol precipitation and analyzed by denaturing 8 to 10% polyacrylamide sequencing gels (45, 46). Labeled RNA bands were visualized by X-ray film autoradiography. Quantitation of the values of the relevant RNA bands was done by the use of the EZQuant-Gel software for densitometric quantitation.

For assembly and purification of initiation complexes of Pol III by velocity sedimentation in glycerol gradient (45), 0.2 mL of whole cell extract (S20) was mixed with 1.25 μg of a human $tRNA^{Arg}$ gene carried on plasmid in 1× assembly buffer [10 mM Tris·HCl, pH 7.9 at 4 °C, 8 mM $MgCl_2$, 20 mM $(NH4)_2SO4$, 5 mM sodium creatine phosphate, 2 mM dithiothreitol (DTT) and 0.5 mM adenosine triphosphate]. The 0.4-mL mixture was then incubated at 30 °C for 10 min for formation of initiation complexes before it was layered on a 4.4-mL volume glycerol gradient prepared in 12 × 51 mm polyallomer tubes placed on ice in a cold room. The gradient was made of 15 to 40% vol/vol glycerol, 20 mM Tris·HCl, pH 7.9, 6 mM $MgCl_2$, 40 mM $(NH4)_2SO4$, 0.2 mM EDTA, pH 8.0 and 2 mM DTT. Centrifugation was executed in an ultracentrifuge

using a TST55.5 rotor at 250,000 × *g* (50,000 rpm) for 3.5 h at 2 °C. Fractions of 0.2 mL in volume were collected from the top of the gradient. Aliquots of 50 μL from selected fractions were immediately examined for Pol III activity in transcription reactions of 55 μL in the presence of 0.5 mM of rNTP and 10 μCi of [α-^{32}P] UTP. Labeled RNAs were then extracted from the reaction mixtures, analyzed by electrophoresis in an 8 to 10% sequencing gel, and quantified, as described above.

Whole Exome Sequencing. Whole exome sequencing was performed on DNA from the patient using the SureSelect Human All Exon V.2 Kit (Agilent Technologies) on HiSeq2000 (Illumina) as 100-bp paired-end runs. Reads alignment and variant calling were performed with DNAnexus software using the default parameters with the human genome assembly hg19 (GRCh37) as a reference.

Data Availability. All relevant data in the paper are entirely available through both text and figures, in the main text and *SI Appendix*.

ACKNOWLEDGMENTS. R.S. and N.O. are grateful for doctoral fellowship support from the Hoffman Leadership and Responsibility Program, the Rudin Foundation, and a Bester Cancer Research Doctoral Fellowship. This research was supported by the United States-Israel Bi-National Science Foundation grant 2015/157 and by the Israel Science Foundation grant 1205/17 to N.J.

1. R. G. Roeder, Nuclear RNA polymerases: Role of general initiation factors and cofactors in eukaryotic transcription. *Methods Enzymol.* **273**, 165–171 (1996).
2. R. G. Roeder, The role of general initiation factors in transcription by RNA polymerase II. *Trends Biochem. Sci.* **21**, 327–335 (1996).
3. L. Schramm, N. Hernandez, Recruitment of RNA polymerase III to its target promoters. *Genes Dev.* **16**, 2593–2620 (2002).
4. G. Dieci, G. Fiorino, M. Castelnuovo, M. Teichmann, A. Pagano, The expanding RNA polymerase III transcriptome. *Trends Genet.* **23**, 614–622 (2007).
5. R. J. White, Transcription by RNA polymerase III: More complex than we thought. *Nat. Rev. Genet.* **12**, 459–463 (2011).
6. R. D. Moir, I. M. Willis, Regulation of pol III transcription by nutrient and stress signaling pathways. *Biochim. Biophys. Acta* **1829**, 361–375 (2013).
7. T. W. Turowski, D. Tollervey, Transcription by RNA polymerase III: Insights into mechanism and regulation. *Biochem. Soc. Trans.* **44**, 1367–1375 (2016).
8. N. A. Hoffmann, A. J. Jakobi, M. K. Vorländer, C. Sachse, C. W. Müller, Transcribing RNA polymerase III observed by electron cryomicroscopy. *FEBS J.* **283**, 2811–2819 (2016).
9. J. Acker, C. Conesa, O. Lefebvre, Yeast RNA polymerase III transcription factors and effectors. *Biochim. Biophys. Acta* **1829**, 283–295 (2013).
10. A. Vannini, P. Cramer, Conservation between the RNA polymerase I, II, and III transcription initiation machineries. *Mol. Cell* **45**, 439–446 (2012).
11. Z. Wang, R. G. Roeder, Three human RNA polymerase III-specific subunits form a subcomplex with a selective function in specific transcription initiation. *Genes Dev.* **11**, 1315–1326 (1997).
12. E. Landrieux *et al*., A subcomplex of RNA polymerase III subunits involved in transcription termination and reinitiation. *EMBO J.* **25**, 118–128 (2006).
13. G. A. Kassavetis, P. Prakash, E. Shim, The C53/C37 subcomplex of RNA polymerase III lies near the active site and participates in promoter opening. *J. Biol. Chem.* **285**, 2695–2706 (2010).
14. C.-C. Wu, Y.-C. Lin, H.-T. Chen, The TFIIF-like Rpc37/53 dimer lies at the center of a protein network to connect TFIIIC, Bdp1, and the RNA polymerase III active center. *Mol. Cell. Biol.* **31**, 2715–2728 (2011).
15. J. G. Dauwerse *et al*., Mutations in genes encoding subunits of RNA polymerases I and III cause Treacher Collins syndrome. *Nat. Genet.* **43**, 20–22 (2011).
16. N. Walker-Kopp *et al*., Treacher Collins syndrome mutations in Saccharomyces cerevisiae destabilize RNA polymerase I and III complex integrity. *Hum. Mol. Genet.* **26**, 4290–4300 (2017).
17. G. Bernard *et al*., Mutations of POLR3A encoding a catalytic subunit of RNA polymerase Pol III cause a recessive hypomyelinating leukodystrophy. *Am. J. Hum. Genet.* **89**, 415–423 (2011).
18. H. Saitsu *et al*., Mutations in POLR3A and POLR3B encoding RNA Polymerase III subunits cause an autosomal-recessive hypomyelinating leukoencephalopathy. *Am. J. Hum. Genet.* **89**, 644–651 (2011).
19. I. Thiffault *et al*., Recessive mutations in POLR1C cause a leukodystrophy by impairing biogenesis of RNA polymerase III. *Nat. Commun.* **6**, 7623 (2015).
20. D. N. Azmanov *et al*., Transcriptome-wide effects of a POLR3A gene mutation in patients with an unusual phenotype of striatal involvement. *Hum. Mol. Genet.* **25**, 4302–4314 (2016).
21. R. Adman, L. D. Schultz, B. D. Hall, Transcription in yeast: Separation and properties of multiple FNA polymerases. *Proc. Natl. Acad. Sci. U.S.A.* **69**, 1702–1706 (1972).
22. V. Thuillier, I. Brun, A. Sentenac, M. Werner, Mutations in the alpha-amanitin conserved domain of the largest subunit of yeast RNA polymerase III affect pausing, RNA cleavage and transcriptional transitions. *EMBO J.* **15**, 618–629 (1996).
23. L. Lama, C. I. Seidl, K. Ryan, New insights into the promoterless transcription of DNA coligo templates by RNA polymerase III. *Transcription* **5**, e27913 (2014).
24. C. I. Seidl, L. Lama, K. Ryan, Circularized synthetic oligodeoxynucleotides serve as promoterless RNA polymerase III templates for small RNA generation in human cells. *Nucleic Acids Res.* **41**, 2552–2564 (2013).
25. A. Ablasser *et al*., RIG-I-dependent sensing of poly(dA:dT) through the induction of an RNA polymerase III-transcribed RNA intermediate. *Nat. Immunol.* **10**, 1065–1072 (2009).
26. Y.-H. Chiu, J. B. Macmillan, Z. J. Chen, RNA polymerase III detects cytosolic DNA and induces type I interferons through the RIG-I pathway. *Cell* **138**, 576–591 (2009).
27. M. Yoneyama *et al*., The RNA helicase RIG-I has an essential function in double-stranded RNA-induced innate antiviral responses. *Nat. Immunol.* **5**, 730–737 (2004).
28. Y.-M. Loo, M. Gale Jr., Immune signaling by RIG-I-like receptors. *Immunity* **34**, 680–692 (2011).
29. D. Ori, M. Murase, T. Kawai, Cytosolic nucleic acid sensors and innate immune regulation. *Int. Rev. Immunol.* **36**, 74–88 (2017).
30. C. Reis e Sousa, Sensing infection and tissue damage. *EMBO Mol. Med.* **9**, 285–288 (2017).
31. E. K. Crill, S. R. Furr-Rogers, I. Marriott, RIG-I is required for VSV-induced cytokine production by murine glia and acts in combination with DAI to initiate responses to HSV-1. *Glia* **63**, 2168–2180 (2015).
32. L. R. H. Ahlers, R. G. Bastos, A. Hiroyasu, A. G. Goodman, Invertebrate iridescent virus 6, a DNA virus, stimulates a mammalian innate immune response through RIG-I-like receptors. *PLoS One* **11**, e0166088 (2016).
33. S. P. Jehl, C. V. Nogueira, X. Zhang, M. N. Starnbach, IFNγ inhibits the cytosolic replication of Shigella flexneri via the cytoplasmic RNA sensor RIG-I. *PLoS Pathog.* **8**, e1002809 (2012).
34. K. Burleigh *et al*., Human DNA-PK activates a STING-independent DNA sensing pathway. *Sci. Immunol.* **5**, eaba4219 (2020).
35. S. Luecke, S. R. Paludan, Molecular requirements for sensing of intracellular microbial nucleic acids by the innate immune system. *Cytokine* **98**, 4–14 (2017).
36. M. Morchikh *et al*., HEXIM1 and NEAT1 long non-coding RNA form a multi-subunit complex that regulates DNA-mediated innate immune response. *Mol. Cell* **67**, 387–399.e5 (2017).
37. B. Ogunjimi *et al*., Inborn errors in RNA polymerase III underlie severe varicella zoster virus infections. *J. Clin. Invest.* **127**, 3543–3556 (2017).
38. M. E. Carter-Timofte, A. F. Hansen, M. Christiansen, S. R. Paludan, T. H. Mogensen, Mutations in RNA Polymerase III genes and defective DNA sensing in adults with varicella-zoster virus CNS infection. *Genes Immun.* **20**, 214–223 (2019).
39. S. Edvardson *et al*., Deleterious mutation in the mitochondrial arginyl-transfer RNA synthetase gene is associated with pontocerebellar hypoplasia. *Am. J. Hum. Genet.* **81**, 857–862 (2007).
40. A. Ta-Shma *et al*., Congenital valvular defects associated with deleterious mutations in the *PLD1* gene. *J. Med. Genet.* **54**, 278–286 (2017).
41. J. M. Schwarz, C. Rödelsperger, M. Schuelke, D. Seelow, MutationTaster evaluates disease-causing potential of sequence alterations. *Nat. Methods* **7**, 575–576 (2010).
42. A. Leaver-Fay *et al*., ROSETTA3: An object-oriented software suite for the simulation and design of macromolecules. *Methods Enzymol.* **487**, 545–574 (2011).
43. N. A. Hoffmann *et al*., Molecular structures of unbound and transcribing RNA polymerase III. *Nature* **528**, 231–236 (2015).
44. J. H. Ou, D. W. Trent, J. H. Strauss, The 3′-non-coding regions of alphavirus RNAs contain repeating sequences. *J. Mol. Biol.* **156**, 719–730 (1982).
45. R. Serruya *et al*., Human RNase P ribonucleoprotein is required for formation of initiation complexes of RNA polymerase III. *Nucleic Acids Res.* **43**, 5442–5450 (2015).
46. R. Reiner, Y. Ben-Asouli, I. Krilovetzky, N. Jarrous, A role for the catalytic ribonucleoprotein RNase P in RNA polymerase III transcription. *Genes Dev.* **20**, 1621–1635 (2006).
47. G. Abascal-Palacios, E. P. Ramsay, F. Beuron, E. Morris, A. Vannini, Structural basis of RNA polymerase III transcription initiation. *Nature* **553**, 301–306 (2018).
48. Y.-Y. Wei, H.-T. Chen, Functions of the TFIIE-related tandem winged-helix domain of Rpc34 in RNA polymerase III initiation and elongation. *Mol. Cell. Biol.* **38**, e00105-17 (2018).
49. A. Grahn, M. Studahl, Varicella-zoster virus infections of the central nervous system–Prognosis, diagnostics and treatment. *J. Infect.* **71**, 281–293 (2015).
50. J. Haroche *et al*., Histiocytoses: Emerging neoplasia behind inflammation. *Lancet Oncol.* **18**, e113–e125 (2017).
51. J. Donadieu, F. Chalard, E. Jeziorski, Medical management of langerhans cell histiocytosis from diagnosis to treatment. *Expert Opin. Pharmacother.* **13**, 1309–1322 (2012).
52. A. R. Schmitt, D. A. Wetter, M. J. Camilleri, S. P. Khan, M. M. Tollefson, Langerhans cell histiocytosis presenting as a blueberry muffin rash. *Lancet* **390**, 155 (2017).
53. G. Badalian-Very, J.-A. Vergilio, M. Fleming, B. J. Rollins, Pathogenesis of Langerhans cell histiocytosis. *Annu. Rev. Pathol.* **8**, 1–20 (2013).
54. G. Badalian-Very *et al*., Recurrent BRAF mutations in Langerhans cell histiocytosis. *Blood* **116**, 1919–1923 (2010).
55. L. Y. Ballester *et al*., The use of BRAF V600E mutation-specific immunohistochemistry in pediatric Langerhans cell histiocytosis. *Hematol. Oncol.* **36**, 307–315 (2018).
56. T. Satoh *et al*., B-RAF mutant alleles associated with Langerhans cell histiocytosis, a granulomatous pediatric disease. *PLoS One* **7**, e33891 (2012). Erratum in: *PLoS One* **7**, 10.1371/annotation/74a67f4e-a536-4b3f-a350-9a4c1e6bebbd (2012).
57. E. Jeziorski *et al*., Herpes-virus infection in patients with langerhans cell histiocytosis: A case-controlled sero-epidemiological study, and in situ analysis. *PLoS One* **3**, e3262 (2008).
58. I. Murakami *et al*., Merkel cell polyomavirus and Langerhans cell neoplasm. *Cell Commun. Signal.* **16**, 49 (2018).
59. C. Nezelof, F. Basset, An hypothesis Langerhans cell histiocytosis: The failure of the immune system to switch from an innate to an adaptive mode. *Pediatr. Blood Cancer* **42**, 398–400 (2004).
60. M. Khalifa, L. Naffaa, Exome sequencing reveals a novel WDR45 frameshift mutation and inherited POLR3A heterozygous variants in a female with a complex phenotype and mixed brain MRI findings. *Eur. J. Med. Genet.* **58**, 381–386 (2015).
61. Y. Weisblum *et al*., Modeling of human cytomegalovirus maternal-fetal transmission in a novel decidual organ culture. *J. Virol.* **85**, 13204–13213 (2011).
62. R. Reiner, N. Krasnov-Yoeli, Y. Dehtiar, N. Jarrous, Function and assembly of a chromatin-associated RNase P that is required for efficient transcription by RNA polymerase I. *PLoS One* **3**, e4072 (2008).